doi:10.5598/imafungus.2015.06.01.14

IMA FUNGUS · 6(1): 215–231 (2015)

ARTICLE

# *Basidioascus undulatus*: genome, origins, and sexuality

Hai D.T. Nguyen[1,2], Denise Chabot[3], Yuuri Hirooka[1,2], Robert W. Roberson[4], and Keith A. Seifert[1,2]

[1]Department of Biology, Faculty of Science, University of Ottawa, 30 Marie Curie, Ottawa, Ontario, K1N 6N5, Canada; corresponding author e-mail: hai.nguyen.1984@gmail.com

[2]Biodiversity (Mycology), Eastern Cereal and Oilseed Research Centre, Agriculture and Agri-Food Canada, 960 Carling Ave., Ottawa, Ontario, K1A 0C6, Canada

[3]Microscopy Centre, Eastern Cereal and Oilseed Research Centre, Agriculture and Agri-Food Canada, 960 Carling Ave., Ottawa, Ontario, K1A 0C6, Canada

[4]School of Life Sciences, Arizona State University, Tempe, AZ 85287-1601, USA

**Abstract:** *Basidioascus undulatus* is a soil basidiomycete belonging to the order *Geminibasidiales*. The taxonomic status of the order was unclear as originally it was only tentatively classified in the class *Wallemiomycetes*. The fungi in *Geminibasidiales* have an ambiguously defined sexual cycle. In this study, we sequenced the genome of *B. undulatus* to gain insights into its sexuality and evolutionary origins. The assembled genome draft was approximately 32 Mb in size, had a median nucleotide coverage of 24X, and contained 6123 predicted genes. Previous morphological descriptions of *B. undulatus* relied on interpretation of putative sexual structures. In this study, nuclear staining and confocal microscopy showed meiosis occurring in basidia and genome analysis confirmed the existence of genes involved in meiosis and mating. Using 35 protein-coding genes extracted from genomic information, phylogenomic and molecular dating analyses confirmed that *B. undulatus* indeed belongs to a lineage distantly related to *Wallemia* while retaining a basal position in *Agaricomycotina*. These results, combined with differences in septal pore morphology, led us to move the order *Geminibasidiales* out of the *Wallemiomycetes* and into the new class *Geminibasidiomycetes* cl. nov. Finally, the concept of *Agaricomycotina* is emended to include both *Wallemiomycetes* and *Geminibasidiomycetes*.

**Key words:**
*Agaricomycotina*
*Basidiomycota*
*Geminibasidiomycetes*
septal pore ultastructure
*Wallemiomycetes*

**Article info:** Submitted: 16 March 2015; Accepted: 13 June 2015; Published: 19 June 2015.

## INTRODUCTION

Using morphological characters, Matsushima (2003) described *Basidioascus undulatus* as the only species in the new genus *Basidioascus* based on a single strain isolated from the tropical rainforest soil in Cape Tribulation National Park, Queensland, Australia. Matsushima (2003) photographed fertile structures of *B. undulatus*, which he interpreted as asci giving rise to ascospores, bearing hooks that could be either croziers or clamps. The genus was named *Basidioascus* after what he interpreted as "basidia-like asci" and the species epithet *undulatus* was given to recall "ascospores with a wavy wall" (Matsushima 2003). Also, *B. undulatus* produced a geotrichum-like asexual morph in culture, characterized by chains of aseptate arthroconidia. MycoBank (Robert *et al.* 2013) and *Ainsworth & Bisby's Dictionary of the Fungi* (Kirk *et al.* 2008) classified *B. undulatus* in *Saccharomycetes* because the asexual morph was assumed to be a *Geotrichum* (a genus typified by an asexual morph and usually associated with sexual morphs in *Galactomyces* or *Dipodascus*).

During a survey of heat resistant fungi in Canadian soils, Nguyen *et al.* (2013) isolated nine additional strains of *B. undulatus*, and a second species of *Basidioascus,* named *B. magus*. A third yeast-like species, *B. persicus*, was recently described from soil in Iran (Nasr *et al.* 2014). Soil appears to be the main habitat for *Basidioascus* species and their distribution is probably broad. However, their ecological role is currently unknown, but they are presumably saprobic as are many soil inhabiting fungi (Domsch *et al.* 1980).

Surprisingly, phylogenetic analyses with rDNA sequences showed that *Basidioascus* was related to *Wallemiomycetes* (*Basidiomycota*) rather than *Saccharomycetes* (*Ascomycota*) (Nguyen *et al.* 2013). This finding initiated a revision of its taxonomy and a re-interpretation of its morphology as a basidiomycete. The structures identified as asci and ascospores by Matsushima (2003) are reinterpretted as thick-walled basidiospores, and the subtending cell as a basidium that usually produces a single basidiospore. Most unusual was that the basidia appeared to be forcibly discharged, leaving them collapsed with the basidiospore still attached by a long, cylindrical sterigma (Nguyen *et al.* 2013). The species of *Basidioascus,* and of its sister genus *Geminibasidium* (*G. donsium* and *G. hirsutum*), were classified in the new order *Geminibasidiales* (Nguyen *et al.* 2013). The *Geminibasidiales* are a phylogenetic sister

group to *Wallemiales* and were placed tentatively under the class *Wallemiomycetes* (Nguyen *et al.* 2013). *Wallemiales* currently includes a single genus *Wallemia* with three species: *W. sebi*, *W. muriae*, and *W. ichthyophaga* (Zalar *et al.* 2005). The phylogenetic placement of *Wallemiomycetes* in the fungal kingdom was at first ambiguous (Matheny *et al.* 2006) because only a few protein coding genes were used in phylogenetic analyses and because ribosomal genes did not provide robustly supported conclusions. However, a few recent studies, through phylogenomic analyses with a large number of protein coding genes, demonstrate that this lineage is an early diverging one within *Agaricomycotina* (Padamsee *et al.* 2012, Zajc *et al.* 2013).

In this study, our first objective was to gain further insight into the sexuality of *B. undulatus* because the structures referred to as basidia and basidiospores were only putatively identified as such (Nguyen *et al.* 2013). For this purpose, we performed nuclear staining on these presumed sexual structures and observed them with laser confocal microscopy. Further, we sequenced the genome of *B. undulatus* and looked for genes involved in meiosis and mating to support our findings. Our second objective was to resolve the tentative placement of *Geminibasidiales* in *Wallemiomycetes*. We conducted phylogenomic analysis using 35 single copy protein-coding genes from the *B. undulatus* genome and we performed a molecular clock analysis to date the divergence of *B. undulatus* from *Wallemia* species and other fungi. The third objective was to investigate the septal pore morphology, which has proved significant in basidiomycete systematics, especially at class rank and particularly in lineages of *Agaricomycotina* (van Driel *et al.* 2009). We imaged the septal pore of *B. undulatus*, *G. donsium,* and *W. sebi* using transmission electron microscopy to support our interpretation of the higher classification of the *Geminibasidiales*.

## MATERIALS AND METHODS

### Growth, DNA extraction and sequencing

The ex-type strain of *Basidioascus undulatus* (DAOM 241956) was inoculated in 2 % malt extract broth in an Erlenmeyer flask on an orbital shaker at 25 °C for 2 wk. The broth culture was transferred to two 50 mL Falcon tubes and centrifuged at 10000 × g for 5 min. The liquid was decanted, leaving only the fungal tissue. The fungal tissue was frozen in liquid nitrogen and crushed with a sterile pestle. DNA was extracted with the OmniPrep kit (G-Biosciences, St Louis, MO) following the manufacturer's instructions. DNA quality and quantity were verified with Qbit (Life Technologies, Burlington, Canada). Whole-genome sequencing (101 base pairs (bp) paired-end) was performed on an Illumina HiSeq 2500 with TrueSeq V3 chemistry at the National Research Council Canada facilty in Saskatoon (Saskatchewan).

### Genome assembly and annotation

The quality of the reads was checked with the program FastQC v. 0.10.1 (http://www.bioinformatics.babraham.ac.uk/projects/fastqc/). Using fastx_trimmer (part of the FASTX-Toolkit v. 0.0.13; http://hannonlab.cshl.edu/fastx_toolkit/), eight bases from the 5' end were trimmed to yield reads of 93 bp in length of higher quality. *De novo* assembly was performed using SPAdes v. 3.0 (Bankevich *et al.* 2012) with the BayesHammer error correction (Nikolenko *et al.* 2013) and mismatch correction enabled (parameters: --careful and k=21, 31, 41, 51, 61, 71, 81, 91). Final contigs were assembled into scaffolds with SSPACE v2.0 (Boetzer *et al.* 2011) (parameters: -x 1 -m 45 -o 10 -t 0 -r 0.7 -k 5 -a 0.7 -n 10 -z 2000 -T 16 -p 1) and contigs shorter than 2000 bp were discarded. Assembly statistics were generated with QUAST v. 2.3 (Gurevich *et al.* 2013). The assembly was checked by aligning the corrected reads onto the scaffolds using Bowtie2 v2.1.0 (Langmead & Salzberg 2012). Alignments produced by Bowtie2 in SAM format were converted to sorted BAM format by SAMtools v. 0.1.19 (Li *et al.* 2009) and statistics for coverage were generated with Qualimap v. 0.8.1 (Garcia-Alcalde *et al.* 2012). To benchmark the completeness of our genome assembly, CEGMA v. 2.5 (Parra *et al.* 2007) was run on the scaffolds to detect the percentage of conserved eukaryotic genes (CEGs).

Genome annotation was performed following established guidelines (Haas *et al.* 2011). Repeats in scaffold sequences were masked with RepeatMasker v. 4.0.5 (http://www.repeatmasker.org) (parameters: -no_is -species fungi) using the Repbase libraries (http://www.girinst.org/). The masked scaffolds were used as input for the MAKER2 v. 2.10 (Holt & Yandell 2011) genome annotation pipeline. In the MAKER2 pipeline, the GeneMark-ES v. 2.3e (Borodovsky & Lomsadze 2011) *ab initio* gene prediction tool was enabled and the NCBI RefSeq protein sequences were aligned to the genome using exonerate v. 2.2.0 (Slater & Birney 2005). Predicted gene models exhibiting strong evidence by exon alignment were exported as protein sequences and coding nucleotide sequences (CDS). Predicted gene models lacking evidence from exon alignment were discarded in downstream analyses. To determine function, the protein sequences were used as input for InterProScan 5RC6 (Jones *et al.* 2014) (parameters: -dp -f -t p -iprlookup -pa -goterms) and were also compared to the manually curated protein data set from UniProt/Swiss-Prot by blastp v. 2.2.28+. The results in XML format from blastp v. 2.2.28+ and InterProScan were loaded into Blast2GO v. 2.7.1 (Conesa *et al.* 2005) and merged to create an annotation table (available from the first author on request). The gene models with BLAST hits having e-value of less than $1.0E^{-100}$ and mean similarity hit of ≥ 70% were assumed to be orthologs and they were given names following recommended conventions (http://www.uniprot.org/docs/proknameprot). Ribosomal RNA's were predicted by RNAmmer v. 1.2 (Lagesen *et al.* 2007). Data files are publicly available at NCBI (Genome Accession No. JTLS00000000 version JTLS01000000; BioProject Accession No. PRJNA247992) and JGI MycoCosm portal (Grigoriev *et al.* 2014).

### Identification of meiosis and mating genes

BLAST was used for finding the *Basidioascus undulatus* mating and meiosis genes. The protein sequences predicted from evidence-supported gene models, determined above, were formatted into a local BLAST database with makeblastdb v. 2.2.28+ (Camacho *et al.* 2009).

Genes previously determined to be involved in meiosis in *Saccharomyces cerevisiae* and *Cryptococcus neoformans*

(Halary *et al.* 2011) were chosen as input queries (e-value cut off < 1.0E$^{-05}$) for the *B. undulatus* protein BLAST database using blastp v. 2.2.28+. *Saccharomyces cerevisiae* and *C. neoformans* were chosen because they are well studied genetically and all meiosis-specific proteins are present (Halary *et al.* 2011).

Mating genes were located with the protein domains identified by InterProScan, and by blastp v. 2.2.28+ using known mating genes in *Saccharomyces cerevisiae* as blastp input queries (e-value cut off < 1.0E$^{-05}$).

## Phylogenomics and molecular dating

Protein sequences of selected fungi (*Agaricus bisporus* var. *bisporus* (H97) v. 2.0 (Morin *et al*. 2012), *Alternaria brassicicola* (Ohm *et al*. 2012), *Arthrobotrys oligospora* ATCC 24927 (Yang *et al*. 2011), *Aureobasidium pullulans* var. *pullulans* EXF-150 (Gostincar *et al*. 2014), *Auricularia subglabra* v. 2.0 (Floudas *et al*. 2012), *Botrytis cinerea* v. 1.0 (Staats and van Kan 2012), *Coccidioides immitis* RS (Sharpton *et al*. 2009), *Coprinopsis cinerea* (Stajich *et al*. 2010), *Cryptococcus neoformans* var. *neoformans* JEC21 (Loftus *et al*. 2005), *Dacryopinax* sp. DJM 731 SSP1 v. 1.0 (Floudas *et al*. 2012), *Fomitiporia mediterranea* v. 1.0 (Floudas *et al*. 2012), *Fomitopsis pinicola* FP-58527 SS1 v. 3.0 (Floudas *et al*. 2012), *Malassezia globosa* (Xu *et al*. 2007), *Mixia osmundae* IAM 14324 v. 1.0 (Toome *et al*. 2014b), *Monacrosporium haptotylum* CBS 200.50 (Meerupati *et al*. 2013), *Neurospora crassa* OR74A v. 2.0 (Galagan *et al*. 2003), *Penicillium chrysogenum* Wisconsin 54-1255 (van den Berg *et al*. 2008), *Puccinia striiformis* f. sp. *tritici* PST-130 (Cantu *et al*. 2011), *Pyronema confluens* CBS 100304 (Traeger *et al*. 2013), *Rhizophagus irregularis* DAOM 181602 v. 1.0 (Tisserant *et al*. 2013), *Saccharomyces cerevisiae* S288C (Goffeau *et al*. 1996), *Sclerotinia sclerotiorum* v. 1.0 (Amselem *et al*. 2011), *Taphrina deformans* (Cisee *et al*. 2013), *Tilletiaria anomala* (Toome *et al*. 2014a), *Tremella mesenterica* Fries v. 1.0 (Floudas *et al*. 2012), *Trichoderma atroviride* v. 2.0 (Kubicek *et al*. 2011), *Tuber melanosporum* (Martin *et al*. 2010), *Ustilago maydis* (Kamper *et al*. 2006), *Wallemia ichthyophaga* EXF-994 (Zajc *et al*. 2013), and *W. sebi* v. 1.0 (Padamsee *et al*. 2012)) were downloaded from the JGI MycoCosm portal (Grigoriev *et al.* 2014) and formatted into separate BLAST databases with makeblastdb v. 2.2.28+. The 246 reliable single copy ortholog protein data set from FUNYbase (Marthey *et al.* 2008) was downloaded. Only amino acid sequences coming from nuclear genes yielding a topological score of > 90 % (Marthey *et al.* 2008) were considered for our phylogenomic analysis (information on exact genes chosen are available from the first author on request). These amino acid sequences were used as blastp v. 2.2.28+ search queries (e-value threshold < 1.0E$^{-05}$) against the protein databases built from data downloaded from JGI MycoCosm described above. Protein sequences were aligned with T-Coffee v10.00.r1613 (Notredame *et al.* 2000) (parameters: t_coffee sequence.fasta -output score_ascii, aln) and poorly aligned regions and columns containing gaps were automatically discarded (parameters: t_coffee -other_pg seq_reformat -in sequence.aln -struc_in sequence.score_ascii -struc_in_f number_aln -action +use_cons +keep '[8-9]' +rm_gap 1 > sequence.best.aln). The alignments were concatenated and converted to PHYLIP format with SeaView v. 4.5.3 (Gouy *et al.* 2010). Three independent phylogenomic analyses were performed with the parallelized version of PhyloBayes 3 (pb_mpi v1.4) (Lartillot *et al.* 2013, Lartillot *et al.* 2009) using the CAT-GTR model (Lartillot & Philippe 2004). Analyses were stopped when convergence was attained (effective size > 100 and maxdiff < 0.1 determined with the programs bpcomp (parameters: -x 1000 50 run1 run2 run3) and tracecomp (parameters: -x 1000 run1 run2 run3), which are part of pb_mpi software package). A lognormal 'relaxed clock' molecular dating analysis was performed with the non-parallelized version of PhyloBayes 3 (pb v3.2e) with a birth-death prior using the tree topology generated from the converged Bayesian analysis above (parameters: -d combined.phy -T bpcomp.con.tre -r outgroup.txt -cal calib.txt -ln -bd md1). *Rhizophagus irregularis* (*Glomeromycota*) was specified as the outgroup. Date constraints previously determined were used as calibrations (Hibbett *et al.* 1997, Smith *et al.* 2004, Taylor & Berbee 2007, Berbee & Taylor 2010, Prieto & Wedin 2013); the exact calibrations are available from the first author on request. Chronograms and statistics were obtained with readdiv (parameters: -x 1000 50 md1), which is part of PhyloBayes 3.

## Confocal laser scanning microscopy

To study nuclear behaviour and to look for indicators of meiosis, *Basidioascus undulatus* DAOM 241956 was grown on corn meal agar (CMA, Acumedia Manufacturers, Lansing, MI) for 1 wk and mounted in DNA stains: DAPI-Fluoromount-G™ mounting medium (EMS, Hatfield, PA) or aqueous SYTO 9 (25 µM) (Life Technologies, Burlington, ON). Samples were visualized under confocal laser scanning microscopy using an LSM 510 DUO (Carl Zeiss MicroImaging, Göttingen, Germany) with a Plan-Apochromat 40×/1.4 Oil DIC objective and electronic zoom 4. An excitation diode laser (405 nm) and emission light (420–700 nm) were used for DAPI. An excitation Argon laser (488 nm) and emission light (505–550 nm) were used for SYTO 9. Images were captured using ZEN 2009 Imaging Software (Carl Zeiss MicroImaging).

## Transmission electron microscopy

Actively growing hyphae of *Basidioascus undulatus* DAOM 241956, *Geminibasidium donsium* DAOM 241966, and *Wallemia sebi* CBS 633.66 were prepared for transmission electron microscopy using cryo-preparation methods. Hyphae were grown on thin, sterile, deionized dialysis membrane segments overlaying appropriate media at 23 ºC. The leading edge of growing mycelia and supporting membranes were trimmed with a sharp razor blade to approximately 5 × 5 mm and after 30–40 min (time to recover from trimming) were removed from the agar surface and immediately cryo-fixed by rapid plunging into liquid propane cooled to –186 ºC with liquid nitrogen (Hoch 1986, Roberson & Fuller 1988, McDaniel & Roberson 2000). After rapid freezing, the samples were freeze-substituted in 1 % glutaraldehyde (w/v) and 1 % tannic acid (w/v) in anhydrous acetone at −85°C for 72 h. After washing in cold acetone (−85 °C), the samples were warmed slowly to room temperature in 1 % $OsO_4$ (w/v) in acetone, washed in acetone, and infiltrated and flat embedded on glass slides in Spurr's resin (Spurr 1969). Using

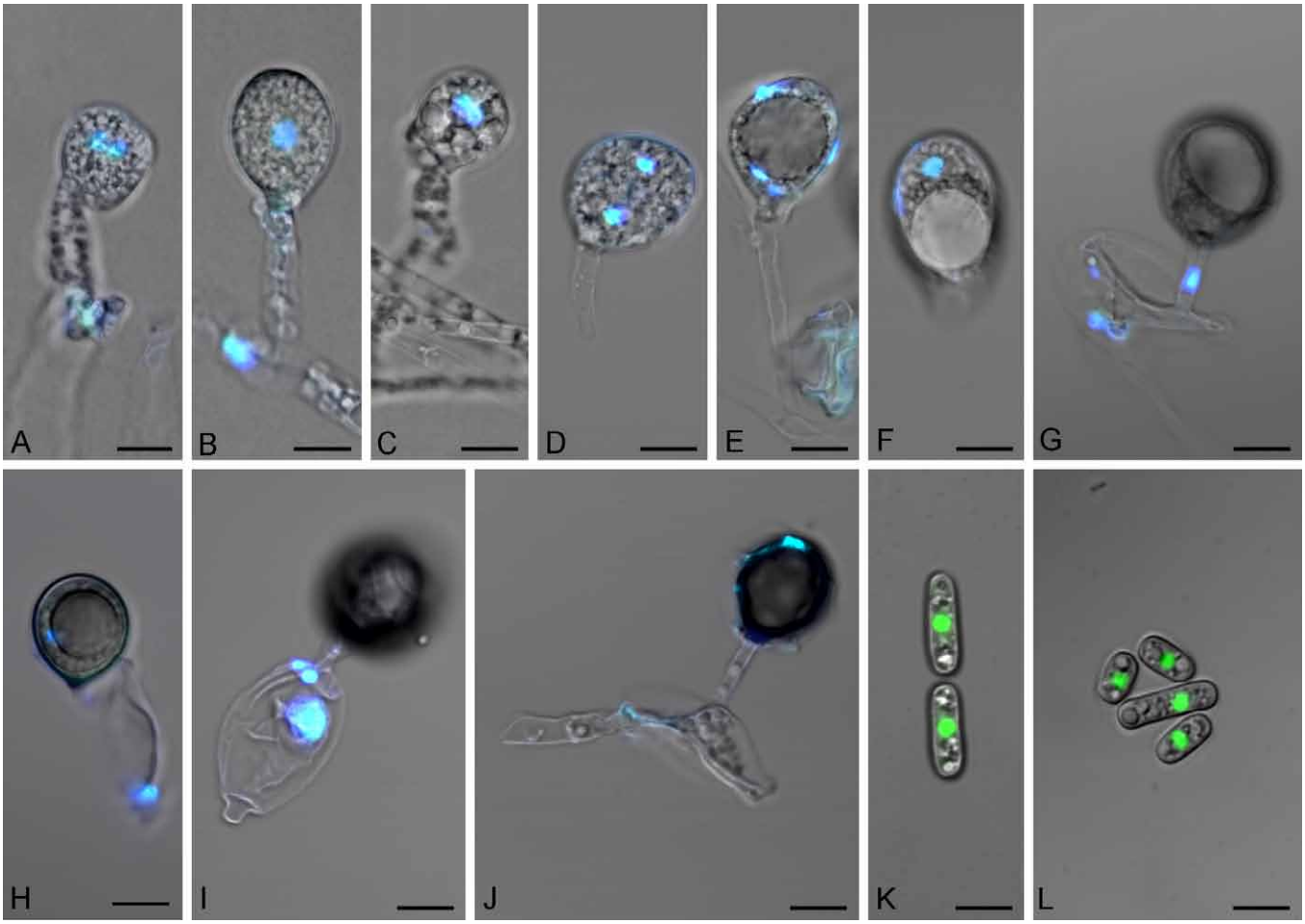


**Fig. 1.** *Basidioascus undulatus* (DAOM 241956) sexual and asexual structures stained with DAPI (A–J) and SYTO 9 (K–L) and imaged with confocal microscopy. **A.** Dikaryotic basidium (2 nuclei). **B.** Karyogamy. **C.** Anaphase I. **D.** Telophase I and collapsed basal lateral projection. **E.** Telophase II (4 nuclei). **F.** Ejected basidium (4 nuclei). **G–H.** Maturation of a basidiospore on a basidium and the migration of a nucleus through the sterigma and into the basidiospore. **I.** Collapsing basidium with the three remaining nuclei. **J.** A totally collapsed basidium and probably one nucleus inside the mature basidiospore. **K–L.** Single nuclei inside arthroconidia. Bar = 5 µm.

phase contrast optics (100×), we examined the slides for well-preserved hyphae and mounted the selected cells on resin blocks (Howard & O'Donnell 1987) then hand-trimmed them. Selected hyphae were sectioned using a Leica Ultracut R ultramicrotome (Leica Microsystems, Bannockburn, IL), collected on copper grids, and post-stained for 10 min in 2 % uranyl acetate in 50 % ethanol and for 5 min in Sato's lead citrate (Hanaichi *et al.* 1986). Sections were then examined using a JEOL 1200EX (JEOL, Tokyo,) transmission electron microscope equipped with a SIA L3C CCD camera (SIA, Duluth, GA). Measurements from captured images were made with ImageJ (Schneider *et al.* 2012).

## RESULTS

### Genome sequencing, assembly and annotation

Short-read Illumina sequencing generated approximately 12 million paired end reads (six million reads in the forward (R1) direction, and six million reads in the reverse (R2) direction) of 101 bp in length each. After trimming to 93 bp, about 1.1 Gb of data was assembled *de novo* to yield a genome assembly size of about 32 Mb. The GC content in *Basidioascus undulatus* was 58 %. The final assembly contained 2992 scaffolds and the longest scaffold was 97 Kb. The nucleotide coverage varied for each scaffold but it was 28X on average and the median nucleotide coverage was 24X. The N50 statistic was 15 Kb. According to CEGMA, 81 % and 88 % of complete and partial CEGs, were detected respectively.

A total of 13935 gene models were detected *ab initio* using GeneMark-ES, but only 6123 gene models were supported by evidence from protein alignment to the NCBI RefSeq fungal protein data. We kept the set of 6123 gene models with evidence for further manual annotation and used it in downstream analyses. Only 3681 of these (60 %) were considered complete because they contained a start and stop codon while the remaining 2442 (40 %) lacked either a start codon, a stop codon, or both.

### Meiosis and meiosis specific genes

To determine whether the putative sexual structures identified by Nguyen *et al.* (2013) truly represented basidia, we followed the fungus's ontogeny and performed nuclear staining by laser confocal microscopy (Fig. 1). Three nuclear divisions normally occur during basidiospore maturation: meiosis

I, meiosis II, followed by four different patterns of post-meiotic mitosis (Duncan & Galbraith 1972). We observed dikaryotic nuclei in the basidia (Fig. 1A), karyogamy (Fig. 1B), anaphase I (Fig. 1C), and the telophase I stage where the basal lateral projection was collapsed (Fig. 1D). Four nuclei from telophase II (Fig. 1E) were seen in both non-discharged and discharged basidia (Fig. 1F). The migration of a nucleus through the sterigma (Fig. 1G) into the basidiospore (Fig. 1H) was observed as the basidiospore matured. There were three remaining nuclei in the collapsing basidium (Fig. 1I) and they eventually degenerated at a later stage when the basidium completely collapsed (Fig. 1J). Whole arthroconidia became stained instead of just their nuclei when DAPI was used. A single nucleus could be spotted in each arthroconidium when stained with SYTO 9 (Fig. 1K–L).

Our microscopic observations correlated with our analysis of the genome to detect meiotic genes (Table 1). All meiosis-specific genes, as defined in Malik *et al.* (2008) and Halary *et al.* (2011), were found in the genome.

## Mating genes

We looked for mating genes such as those encoding for homeodomain proteins, G-protein coupled pheromone receptor, high mobility group (HMG) DNA binding proteins, mitogen-activated protein kinases (MAPK, MAPKK, MAPKKK) and the subunits of the trimeric GTPase protein (Gα, Gβ, Gγ) (James *et al.* 2013). We followed the *Saccharomyces cerevisiae* standard for gene names. Most of the mating response genes and the pheromone processing genes (Table 2) were detected in the *B. undulatus* genome. All of the mating genes detected were located on different scaffolds, except for *KSS*1 and *FUS*3, which co-occurred on scaffold 2837. The presence of most mating genes suggests that a mating type locus exists, but its structure and gene order could not be determined because our assembled genome was too fragmented.

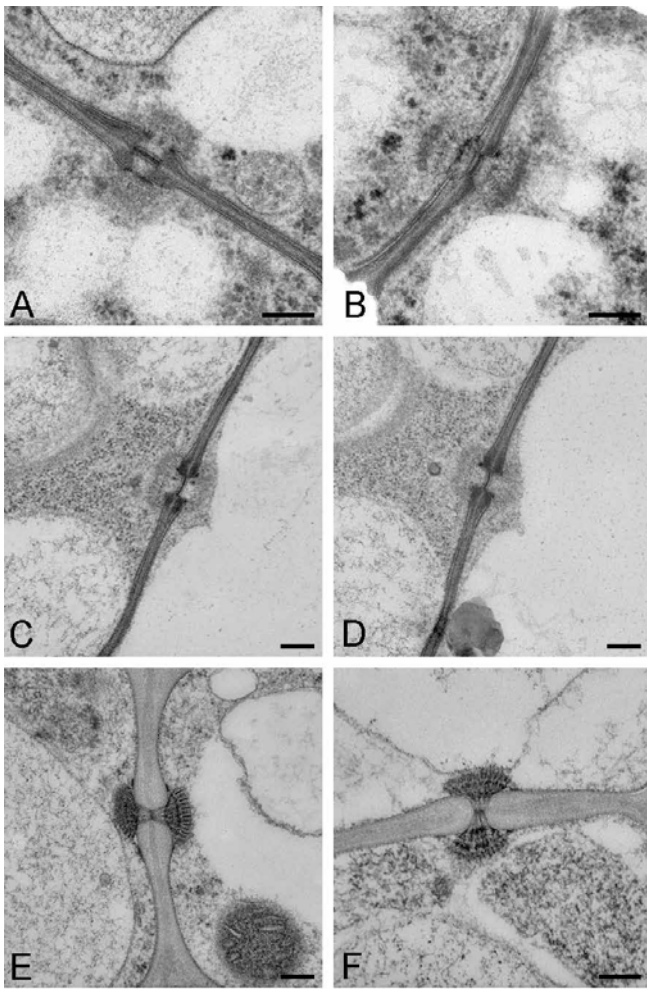


**Fig. 2.** Transmission electron micrographs showing septal pore morphology. **A–B.** *Basidioascus undulatus* (DAOM 241956 ex-type). **C–D.** *Geminibasidium donsium* (DAOM 241966 ex-type). **E–F**. *Wallemia sebi* (CBS 633.66). Bar = 20 µm.

## Septal pore morphology

We imaged the septal pores of *Wallemia sebi*, *Basidioascus undulatus,* and *Gemmibasidium donsium*, all currently classified in *Wallemiomycetes*, using identical fixation methods to strengthen comparisons (Fig. 2). *Basidioascus undulatus, G. donsium* and *W. sebi* all have a dolipore septum characteristic of *Agaricomycotina*. The pore swelling of *B. undulatus* and *G. donsium* is electron dense, but is not in *W. sebi*. The adseptal tubular extensions that arise from sheets of endoplasmic reticulum in *W. sebi* were obvious (Fig. 2E–F) but they were either absent or unclear in *B. undulatus* (Fig. 2A–B) and *G. donsium* (Fig. 2C–D). Electron-dense regions were evident near the septal pore in all three fungi, but this area was denser in *W. sebi* than in *B. undulatus* and *G. donsium*. An electron-dense septal pore occlusion extending across the septal pore was observed in all three fungi. This occlusion was non-membranous in *W. sebi*, which agrees with previously published findings (Terracina 1974, Padamsee *et al.* 2012) and the *W. sebi* data on the AFTOL Structural and Biochemical Database (Celio *et al.* 2007). The septal pore occlusion in *B. undulatus* and *G. donsium* had a membrane, making it more clearly defined compared to that of *W. sebi*. Furthermore, this occlusion was almost twice as wide in *B. undulatus* and *G. donsium* (~0.12 µm) compared with *W. sebi* (~0.06 µm). Also, the septal pore of *W. sebi* had striations that appeared to be fine fibrils vertically arranged at the pore opening, but these were absent in *B. undulatus* and *G. donsium*. We did not see a septal pore cap in our sections of *W. sebi*, *B. undulatus* or *G. donsium*.

## Phylogenomic analysis and molecular dating

Because *Basidioascus* is currently classified in *Wallemiomycetes*, and the phylogenetic position of the fungi classified in this class has been unstable in different analyses as a result of sparse taxon sampling, low gene sampling and conflicts in certain genealogies (Zalar *et al.* 2005, Matheny *et al.* 2006), we performed a phylogenomic analysis using protein sequences from 35 single copy protein-coding genes to study its phylogenetic position in a more robust fashion (Fig. 3A). Our results were similar to those obtained from the rDNA phylogenetic analysis in Nguyen *et al.* (2013), showing *Basidioascus* as a distant lineage to *Wallemia*, with a posterior probability of 1.00. The results were also similar to those of Padamsee *et al.* (2012) and Zajc *et al.* (2013), where

**Table 1.** List of known and putative meiosis genes in the genome of *Saccharomyces cerevisiae*, *Cryptococcus neoformans* and *Basidioascus undulatus*. Meiosis specific proteins are highlighted in red.

| Process | Gene name | *Saccharomyces cerevisiae*[a] | *Cryptococcus neoformans*[b] | *Basidioascus undulatus* vs. *Saccharomyces cerevisiae* | | | | | *Basidioascus undulatus* vs. *Cryptococcus neoformans* | | | | | *Basidioascus undulatus* |
|---|---|---|---|---|---|---|---|---|---|---|---|---|---|---|
| | | Locus ID | | Locus ID | Score | E-value | % identity | % positive | Locus ID | Score | E-value | % identity | % positive | Probable Locus ID |
| **DSB generation** | SPO11 | YHL022C | XM_767420.1 | 102794F55C | 72.8 | 0.0 | 25.46 | 43.54 | 102794F55C | 191 | 0.0 | 32.92 | 51.49 | **102794F55C** |
| | REC107/MEI2 | YJR021C | Absent | Not detected | | | | | NA | | | | | Absent or not detected |
| | MEI4 | YER044C | Absent | Not detected | | | | | NA | | | | | Absent or not detected |
| | REC102 | YLR329W | Absent | Not detected | | | | | NA | | | | | Absent or not detected |
| | REC104 | YHR157W | Absent | Not detected | | | | | NA | | | | | Absent or not detected |
| | REC114 | YMR133W | Absent | Not detected | | | | | NA | | | | | Absent or not detected |
| | SKI8 | YGL213C | XP_567964.1 | Not detected | | | | | A5C17B7D33 | 79.3 | 0.0 | 40 | 54.29 | A5C17B7D33 |
| | MER1 | YNL210W | Absent | Not detected | | | | | NA | | | | | Absent or not detected |
| | HFM1/MER3 | YGL251C | XP_774045.1 | 268E1B92EF | 286 | 0.0 | 30.69 | 50.14 | 268E1B92EF | 285 | 0.0 | 29.55 | 48.66 | **268E1B92EF** |
| | NAM8/MRE2 | YHR086W | XP_568215.1 | 012CC612A1 | 88.6 | 0.0 | 27.24 | 46.24 | C3284824DB | 211 | 0.0 | 75.57 | 83.21 | Conflict |
| **Removal of** | MRE11 | YMR224C | XP_571170.1 | 550A163039 | 365 | 0.0 | 40.59 | 58.02 | 550A163039 | 629 | 0 | 56.55 | 74.34 | **550A163039** |
| **Spo11** | RAD50 | YNL250W | XP_771929.1 | 1CAAD52FF0 | 543 | 0.0 | 30.88 | 52.16 | 1CAAD52FF0 | 869 | 0 | 38.91 | 61.16 | **1CAAD52FF0** |
| | XRS2/NBS1 | YDR369C | Absent | Not detected | | | | | NA | | | | | Absent or not detected |
| | SAE2/COM1 | YGL175C | Absent | Not detected | | | | | NA | | | | | Absent or not detected |
| **Strand invasion** | RAD51 | YER095W | XP_567016.1 | D36F2DAE01 | 481 | 0.0 | 69.28 | 85.58 | D36F2DAE01 | 533 | 0 | 77.71 | 84.46 | **D36F2DAE01** |
| | DMC1 | YER179W | XP_772121.1 | 1B6A6FD704 | 376 | 0.0 | 58.13 | 75.94 | 1B6A6FD704 | 388 | 0.0 | 67.13 | 80.28 | **1B6A6FD704** |
| | RAD52 | YML032C | XP_569087.1 | EA2B481C23 | 186 | 0.0 | 51.9 | 74.05 | EA2B481C23 | 237 | 0.0 | 60.57 | 78.29 | **EA2B481C23** |
| | RAD54 | YGL163C | XP_570462.1 | 4E6C655AE5 | 525 | 0.0 | 61.26 | 78.21 | 4E6C655AE5 | 599 | 0 | 71.22 | 82.93 | **4E6C655AE5** |
| | RDH54 | YBR073W | Absent | ED83E37023 | 476 | 0.0 | 42.43 | 60.41 | NA | | | | | ED83E37023 |
| | RFA1 | YAR007C | XP_775959.1 | 1512E55FF2 | 350 | 0.0 | 41.02 | 62.08 | 1512E55FF2 | 489 | 0.0 | 51.93 | 70.39 | **1512E55FF2** |
| | RFA2 | YNL312W | XP_776149.1 | C06D199EC7 | 95.9 | 0.0 | 37.78 | 55.56 | C06D199EC7 | 174 | 0.0 | 40.51 | 61.18 | **C06D199EC7** |
| | RFA3 | YJL173C | Absent | Not detected | | | | | NA | | | | | Absent or not detected |
| | SAE3 | YHR079C-A | Absent | Not detected | | | | | NA | | | | | Absent or not detected |
| | RAD55 | YDR076W | Absent | Not detected | | | | | NA | | | | | Absent or not detected |
| **DNA damage** | PCH2 | YBR186W | XP_567632.1 | 1586D154C9 | 177 | 0.0 | 36.88 | 53.49 | 1586D154C9 | 418 | 0.0 | 47.79 | 66.81 | **1586D154C9** |
| **checkpoint** | MEC1 | YBR136W | XP_568889.1 | E568B50733 | 483 | 0.0 | 24.05 | 43.61 | 87D911C03D | 713 | 0 | 61.72 | 76.24 | Conflict |
| | RAD17 | YOR368W | XP_569244.1 | Not detected | | | | | D5120AB0E3 | 171 | 0.0 | 34.76 | 48.66 | D5120AB0E3 |
| | RAD24 | YER173W | Absent | D5120AB0E3 | 54.3 | 0.000 | 27.48 | 43.51 | NA | | | | | D5120AB0E3 |
| | DDC1 | YPL194W | Absent | Not detected | | | | | NA | | | | | Absent or not detected |
| **Regulation of** | MLH1 | YMR167W | XP_571158.1 | F0BB260AD1 | 361 | 0.0 | 53.03 | 70.03 | F0BB260AD1 | 642 | 0 | 51.99 | 66.51 | **F0BB260AD1** |
| **crossover** | MLH3 | YPL164C | XP_570272.1 | BC2D40152B | 115 | 0.0 | 23.47 | 44.13 | BC2D40152B | 178 | 0.0 | 37.67 | 57.88 | **BC2D40152B** |
| **frequency** | MSH4 | YFL003C | XP_773414.1 | CAE76A5567 | 347 | 0.0 | 31.07 | 50.64 | CAE76A5567 | 546 | 0 | 39.76 | 59.04 | **CAE76A5567** |
| | MSH5 | YDL154W | XP_566842.1 | A5F9B81D55 | 304 | 0.0 | 30.46 | 52.12 | A5F9B81D55 | 436 | 0.0 | 39.91 | 58.36 | **A5F9B81D55** |

**Table 1.** (Continued).

| Process | Gene name | *Saccharomyces cerevisiae*[a] | *Cryptococcus neoformans*[b] | *Basidioascus undulatus* vs. *Saccharomyces cerevisiae* | | | | | *Basidioascus undulatus* vs. *Cryptococcus neoformans* | | | | | *Basidioascus undulatus* |
|---|---|---|---|---|---|---|---|---|---|---|---|---|---|---|
| | | Locus ID | | Locus ID | Score | E-value | % identity | % positive | Locus ID | Score | E-value | % identity | % positive | Probable Locus ID |
| | SGS1 | YMR190C | XP_776787.1 | FAB5DF8B5F | 526 | 0.0 | 45.14 | 64.24 | FAB5DF8B5F | 597 | 0 | 43.47 | 60.52 | **FAB5DF8B5F** |
| | MEI5 | YPL121C | Absent | Not detected | | | | | NA | | | | | Absent or not detected |
| | MUM2 | YBR057C | Absent | Not detected | | | | | NA | | | | | Absent or not detected |
| | NDJ1 | YOL104C | Absent | Not detected | | | | | NA | | | | | Absent or not detected |
| | RAD1 | YPL022W | XP_772313.1 | 29F5BE17B9 | 258 | 0.0 | 33.14 | 50.95 | 29F5BE17B9 | 374 | 0.0 | 40.1 | 56.48 | **29F5BE17B9** |
| | Rad2 | YGR258C | XP_566738.1 | 41955FBDBD | 248 | 0.0 | 44.04 | 67.51 | 41955FBDBD | 355 | 0.0 | 54.75 | 70.82 | **41955FBDBD** |
| **Synaptonemal** | HOP1 | YIL072W | 50255507 | D659917BB2 | 141 | 0.0 | 31.54 | 56.54 | D659917BB2 | 170 | 0.0 | 34.16 | 50 | **D659917BB2** |
| **complex** | HOP2 | YGL033W | 50255433 | Not detected | | | | | Not detected | | | | | Absent or not detected |
| | MND1 | YGL183C | XP_772550.1 | 5756414F12 | 62 | 0.0 | 20.94 | 43.59 | 5756414F12 | 115 | 0.0 | 37.13 | 51.05 | **5756414F12** |
| | ZIP1 | YDR285W | Absent | 2C075CC8D6 | 204 | 0.0 | 79.7 | 86.47 | NA | | | | | 2C075CC8D6 |
| | ZIP2 | YGL249W | Absent | Not detected | | | | | NA | | | | | Absent or not detected |
| | ZIP3 | YLR394W | Absent | Not detected | | | | | NA | | | | | Absent or not detected |
| | Zip4/Spo22 | YIL073C | 134115038 | Not detected | | | | | Not detected | | | | | Absent or not detected |
| **DNA Repair** | HTA1 | YDR225W | XP_567962.1 | 2C075CC8D6 | 204 | 0.0 | 79.7 | 86.47 | 2C075CC8D6 | 130 | 0.0 | 57.98 | 73.11 | **2C075CC8D6** |
| | HTA2 | YBL003C | XP_569065.1 | 2C075CC8D6 | 206 | 0.0 | 80.45 | 87.22 | F84A4F188E | 205 | 0.0 | 79.39 | 87.79 | Conflict |
| | RED1 | YLR263W | Absent | Not detected | | | | | NA | | | | | Absent or not detected |
| | SMC5 | YOL034W | XP_570071.1 | 8388BCCBA3 | 362 | 0.0 | 27.24 | 48.17 | 8388BCCBA3 | 529 | 0.0 | 32.52 | 51.9 | **8388BCCBA3** |
| | SMC6 | YLR383W | XP_775824.1 | 13E0CFCD07 | 340 | 0.0 | 27.58 | 47.32 | 13E0CFCD07 | 476 | 0.0 | 29.98 | 50.65 | **13E0CFCD07** |
| | EXO1 | YOR033C | XP_777034.1 | 36DFC1EC56 | 276 | 0.0 | 43.67 | 65.33 | 36DFC1EC56 | 389 | 0.0 | 54.49 | 71.07 | **36DFC1EC56** |
| | HRR25 | YPL204W | XP_570121.1 | 22D0CDA5D9 | 464 | 0.0 | 65.33 | 83.28 | 22D0CDA5D9 | 594 | 0 | 95.22 | 98.63 | **22D0CDA5D9** |
| | RAD23 | YEL037C | XP_777611.1 | 0FBB054DC3 | 54.7 | 0.000 | 40.54 | 60.81 | 0FBB054DC3 | 91.3 | 0.0 | 60.81 | 78.38 | **0FBB054DC3** |
| **Mismatch repair** | MSH2 | YOL090W | XP_567098.1 | E449052477 | 746 | 0 | 43.93 | 63.77 | E449052477 | 1087 | 0 | 58.26 | 73.21 | **E449052477** |
| | MSH3 | YCR092C | XP_569494.1 | 7F6ED5B406 | 354 | 0.0 | 29.13 | 49.57 | 7F6ED5B406 | 790 | 0 | 45.31 | 65.61 | **7F6ED5B406** |
| | MSH6 | YDR097C | XP_772722.1 | 122F99619E | 672 | 0 | 36.44 | 56.87 | 122F99619E | 1026 | 0 | 51.24 | 66.83 | **122F99619E** |
| | MLH2 | YLR035C | Absent | 8C03A290CE | 86.7 | 0.0 | 31.93 | 53.61 | NA | | | | | 8C03A290CE |
| | PMS1 | YNL082W | 57225775 | 8C03A290CE | 176 | 0.0 | 48.65 | 67.03 | 8C03A290CE | 236 | 0.0 | 60.51 | 75.38 | **8C03A290CE** |
| **Resolution of** | MMS4 | YBR098W | 58260752 | Not detected | | | | | Not detected | | | | | Not detected or absent |
| **recombination** | MUS81 | YDR386W | XP_777360.1 | E55E7AB0BD | 84 | 0.0 | 30.49 | 49.78 | E55E7AB0BD | 101 | 0.0 | 32.39 | 50.7 | **E55E7AB0BD** |
| **intermediates** | SLX1 | YBR228W | XP_567159.1 | A74C037F01 | 83.2 | 0.0 | 52.44 | 68.29 | A74C037F01 | 108 | 0.0 | 61.54 | 74.36 | **A74C037F01** |
| | TOP1 | YOL006C | XP_572925.1 | DB366D3081 | 439 | 0.0 | 49.78 | 66.89 | DB366D3081 | 518 | 0.0 | 56.71 | 70.56 | **DB366D3081** |
| | TOP2 | YNL088W | XP_566700.1 | 4AE1080675 | 1197 | 0 | 52.97 | 71.47 | 4AE1080675 | 1491 | 0 | 66.48 | 79.24 | **4AE1080675** |
| | TOP3 | YLR234W | XP_773035.1 | BCF17A4E2A | 266 | 0.0 | 43.67 | 60.54 | BCF17A4E2A | 518 | 0.0 | 57.95 | 70.91 | **BCF17A4E2A** |
| | SLX4 | YLR135W | Absent | Not detected | | | | | | | | | | Not detected or absent |

**Table 1.** (Continued).

| Process | Gene name | *Saccharomyces cerevisiae*[a] | *Cryptococcus neoformans*[b] | *Basidioascus undulatus* vs. *Saccharomyces cerevisiae* | | | | | *Basidioascus undulatus* vs. *Cryptococcus neoformans* | | | | | *Basidioascus undulatus* |
|---|---|---|---|---|---|---|---|---|---|---|---|---|---|---|
| | | Locus ID | | Locus ID | Score | E-value | % identity | % positive | Locus ID | Score | E-value | % identity | % positive | Probable Locus ID |
| | SLX5 | YDL013W | Absent | Not detected | | | | | | | | | | Not detected or absent |
| | SLX8 | YER116C | Absent | 52369A1C42 | 52.4 | 0.000 | 35.9 | 48.72 | | | | | | 52369A1C42 |
| **Nonhomologous** | YKU70 | YMR284W | XP_573016.1 | AD4E738F04 | 115 | 0.0 | 24.21 | 42.14 | AD4E738F04 | 228 | 0.0 | 32.28 | 47.76 | **AD4E738F04** |
| **end joining** | YKU80 | YMR106C | XP_568810.1 | 1FC448F440 | 60.8 | 0.000 | 30.29 | 48.57 | 1FC448F440 | 241 | 0.0 | 28.83 | 46.23 | **1FC448F440** |
| | DNL4 | YOR005C | XP_572602.1 | 9206958189 | 223 | 0.0 | 27.5 | 43.38 | E8D29BB570 | 902 | 0 | 71.5 | 83.49 | Conflict |
| | LIF1 | YGL090W | Absent | Not detected | | | | | NA | | | | | Absent or not detected |
| **Other** | MSC1 | YML128C | XP_570348.1 | 6453C9DC91 | 53.1 | 0.000 | 22.02 | 45.83 | 6453C9DC91 | 168 | 0.0 | 34.33 | 51.12 | **6453C9DC91** |
| | MSC7 | YHR039C | XP_773481.1 | AE68F812D8 | 179 | 0.0 | 26.57 | 46.65 | AE68F812D8 | 185 | 0.0 | 28.6 | 45.59 | **AE68F812D8** |
| | MSC3 | YLR219W | Absent | Not detected | | | | | NA | | | | | Absent or not detected |
| | MSC6 | YOR354C | Absent | Not detected | | | | | NA | | | | | Absent or not detected |
| | SRS2 | YJL092W | Absent | C8820A864B | 273 | 0.0 | 28.95 | 44.65 | NA | | | | | C8820A864B |
| | MPS3 | YJL019W | Absent | Not detected | | | | | NA | | | | | Absent or not detected |
| | REC8 | YPR007C | 134090540 | Not detected | | | | | 130D4D9937 | 65.1 | 0.0 | 38.04 | 59.78 | 130D4D9937 |
| | Mcd1/Rad21 | 6320201[b] | 58266400 | 130D4D9937 | 68.6 | 0.0 | 35.05 | 57.73 | 130D4D9937 | 142 | 0.0 | 32.61 | 46.65 | **130D4D9937** |
| | SMC1 | BAA09230.1[b] | XP_568851.1 | 82DC381A41 | 534 | 0.0 | 31.89 | 54.54 | 82DC381A41 | 894 | 0 | 44.85 | 64.74 | **82DC381A41** |
| | SMC2 | P38989.1[b] | XP_572171.1 | 68E0241B20 | 516 | 0.0 | 42.44 | 63.29 | 68E0241B20 | 720 | 0 | 58.48 | 70.98 | **68E0241B20** |
| | SMC3 | CAA74655.1[b] | XP_570201.1 | 10D8B5FBE4 | 248 | 0.0 | 41.53 | 60.17 | 10D8B5FBE4 | 404 | 0.0 | 57.95 | 72.56 | **10D8B5FBE4** |
| | SMC4* | EDV09389.1[b] | XP_571168.1 | C71F05C621 | 895 | 0 | 41.41 | 60.31 | C71F05C621 | 1367 | 0 | 56.6 | 73.61 | **C71F05C621** |
| | SCC3 | P40541.1[b] | XP_567136.1 | Not detected | | | | | Not detected | | | | | Absent or not detected |
| | PDS5 | Q04264.1[b] | XP_567466.1 | 062A151CC3 | 326 | 0.0 | 24.85 | 45.12 | 062A151CC3 | 681 | 0 | 35.27 | 55.63 | **062A151CC3** |

[a] These LocusID's are from *Saccharomyces* Genome Database (http://www.yeastgenome.org/).

[b] These LocusID's are from NCBI Protein database (http://www.ncbi.nlm.nih.gov/protein/).

**Table 2.** List of mating genes.

| Process | Gene name | *Saccharomyces cerevisiae*[a] | *Basidioascus undulatus* vs. *Saccharomyces cerevisiae* | | | | |
|---|---|---|---|---|---|---|---|
| | | Locus ID | Locus ID | Score | E-value | % identity | % positive |
| **Mating response** | STE3 | YKL178C | 601070A992 | 84.7 | 0.0 | 25.17 | 44.37 |
| | KSS1 | YGR040W | 03DD35A234 | 341 | 0.0 | 58.5 | 72.45 |
| | FUS3 | YBL016W | 03DD35A234 | 355 | 0.0 | 57.48 | 74.83 |
| | STE7 | YDL159W | C56EA11F93 | 209 | 0.0 | 49.32 | 66.06 |
| | STE11 | YLR362W | A726A87E58 | 319 | 0.0 | 52.6 | 67.86 |
| | GPA1 | YHR005C | 00D128FF38 | 243 | 0.0 | 55 | 75.5 |
| | STE4 | YOR212W | 51579617AB | 195 | 0.0 | 43.67 | 61.22 |
| | STE18 | YJR086W | Not detected | | | | |
| | STE20 | YHL007C | ABF41DDAEF | 375 | 0.0 | 59.26 | 76.09 |
| | STE12 | YHR084W | Not detected | | | | |
| | FAR1 | YJL157C | Not detected | | | | |
| | STE5 | YDR103W | Not detected | | | | |
| **Pheromone processing** | KEX1 | YGL203C | C1EB8324D8 | 249 | 0.0 | 34.79 | 51.2 |
| | KEX2 | YNL238W | 1DAB65F8AC | 480 | 0.0 | 47.45 | 63.53 |
| | STE13 | YOR219C | C51BE5DE56 | 131 | 0.0 | 42.11 | 63.16 |
| | RAM1 | YDL090C | B544DBFB4B | 169 | 0.0 | 37.09 | 53.31 |
| | RAM2 | YKL019W | B2B303A077 | 82.4 | 0.0 | 30.73 | 45.31 |
| | RCE1 | YMR274C | Not detected | | | | |
| | STE24 | YJR117W | Not detected | | | | |
| | STE14 | YDR410C | CC90F4A946 | 99.8 | 0.0 | 45.45 | 58.68 |
| | AXL1 | YPR122W | 98D2221B58 | 129 | 0.0 | 30.38 | 51.9 |
| | STE6 | YKL209C | ED8249ED54 | 359 | 0.0 | 25.6 | 43.36 |

a: These LocusID's are from *Saccharomyces* Genome Database (http://www.yeastgenome.org/).

the *Wallemiomycetes* were shown to be an early diverging lineage of *Agaricomycotina*.

We dated the divergence of *Basidioascus* from other lineages using some reliable fossil data of basidiomycetes (Hibbett *et al.* 1997, Smith *et al.* 2004) and the latest calculated calibration points (Berbee & Taylor 2010, Prieto & Wedin 2013) (Fig. 3B). Under these assumptions, the split between *B. undulatus* and *Wallemia* was estimated at 250±29 Mya, and that between *W. sebi* and *W. ichthyophaga* was about 33±6 Mya.

## DISCUSSION

### Genome sequencing and annotation

*Basidioascus undulatus* is the first fungus in *Geminibasidiales* with a sequenced genome. The 1.1 Gb of sequence data gave a median nucleotide coverage of 24X and a final assembly that contained 2992 scaffolds, which is similar to what has been produced in many recent whole genome sequencing studies (e.g. Sims *et al.* 2014). *Wallemia sebi* and *W. ichthyophaga* were the closest known relatives to *B. undulatus*. Despite being considered close relatives, the genome assembly size of *B. undulatus* (32 Mb) was larger than *W. sebi* (9.8 Mb) (Padamsee *et al.* 2012) and *W. ichthyophaga* (9.6 Mb) (Zajc *et al.* 2013). Also, the GC content of *B. undulatus* was higher (58 %) compared to *W. sebi* (40 %) and *W. ichthyophaga* (45 %) (Table 3). Based on these results, the fungi of these two genera are more distantly related than initially suspected.

We were able to detect 88 % of partial core eukaryotic genes (CEGs). We assumed that downstream annotation with this genome assembly should, in theory, reveal close to the same proportion of the total number of genes contained in *B. undulatus.*

Many gene prediction tools are available, but GeneMark-ES was selected because it was shown previously to be accurate at detecting genes in fungal genomes (Ter-Hovhannisyan *et al.* 2008). GeneMark-ES considers branch point sequences in the intron model, which guides lariat formation during splicing, providing greater accuracy at locating intron boundaries. Because RNA data were not acquired in our study, we chose to use GeneMark-ES, which does not require RNA data for algorithm training. Nevertheless, genome annotation based on genome sequences alone has limitations. First, without RNA data, CDS predictions cannot be validated and genes from splice sites that use donor and acceptor sequences other than the canonical GT–AG introns cannot be predicted. The frequencies of the non-canonical GC–AG introns are 1.0–1.2 % in some ascomycetes (Rep *et al.* 2006) and could be as high as 3 % in basidiomycetes (Misiek & Hoffmeister 2008). To compensate for the absence of RNA data, the fungal NCBI RefSeq protein sequence data set (13 March 2014 release), which contains curated

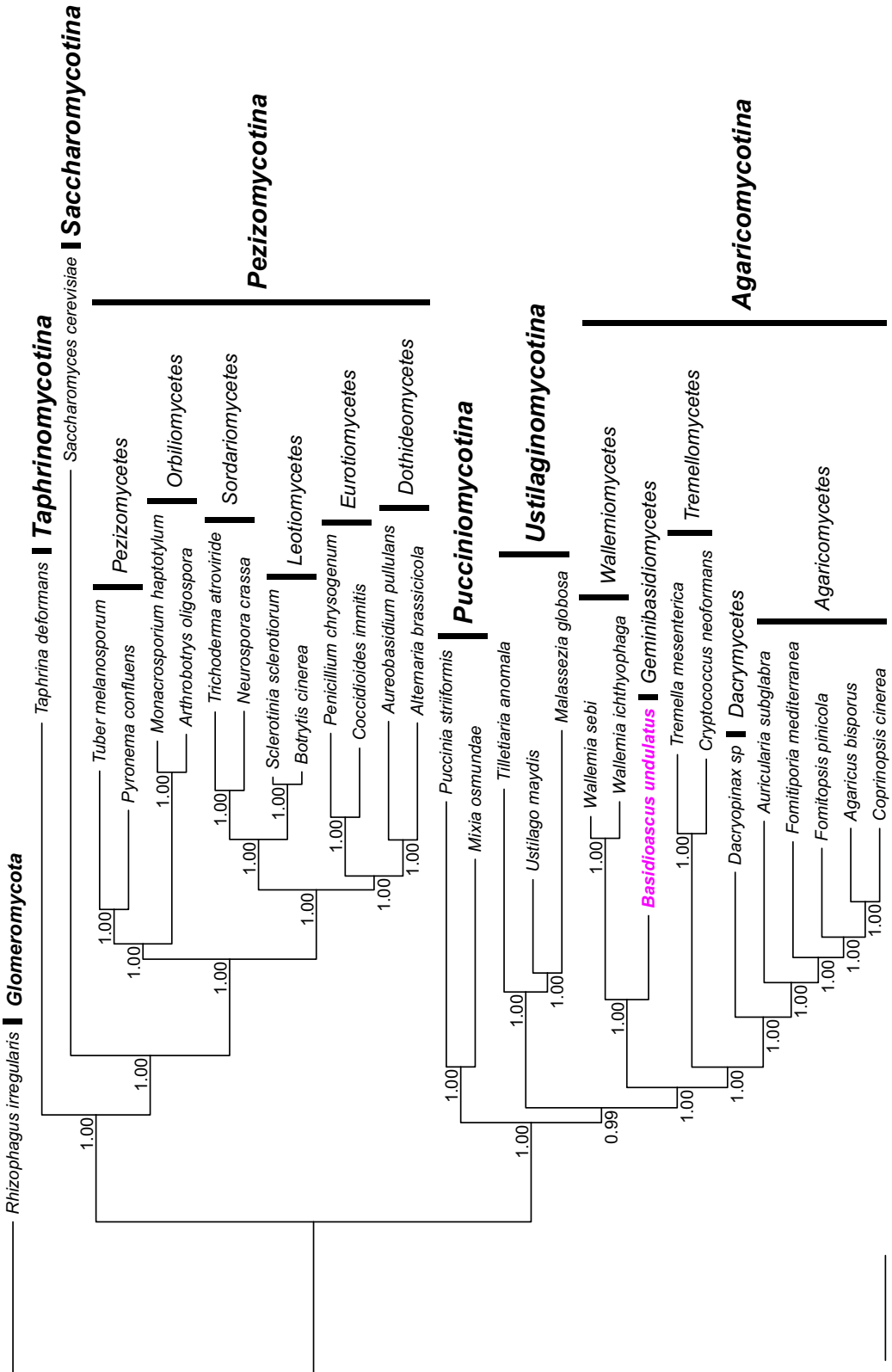
A
Rhizophagus irregularis
Glomeromycota
Taphrina deformans
Taphrinomycotina
Saccharomyces cerevisiae
Saccharomycotina
Tuber melanosporum
Pyronema confluens
Pezizomycetes
Monacrosporium haptotylum
Arthrobotrys oligospora
Orbiliomycetes
Trichoderma atroviride
Neurospora crassa
Sordariomycetes
Sclerotinia sclerotiorum
Botrytis cinerea
Leotiomycetes
Penicillium chrysogenum
Coccidioides immitis
Eurotiomycetes
Aureobasidium pullulans
Altemaria brassicicola
Dothideomycetes
Pezizomycotina
Puccinia striiformis
Mixia osmundae
Pucciniomycotina
Tilletiaria anomala
Ustilago maydis
Ustilaginomycotina
Malassezia globosa
Wallemia sebi
Wallemia ichthyophaga
Wallemiomycetes
Basidioascus undulatus
Geminibasidiomycetes
Tremella mesenterica
Cryptococcus neoformans
Tremellomycetes
Dacryopinax sp
Dacrymycetes
Auricularia subglabra
Fomitiporia mediterranea
Fomitopsis pinicola
Agaricomycetes
Agaricus bisporus
Coprinopsis cinerea
Agaricomycotina
1.00
0.99
0.2

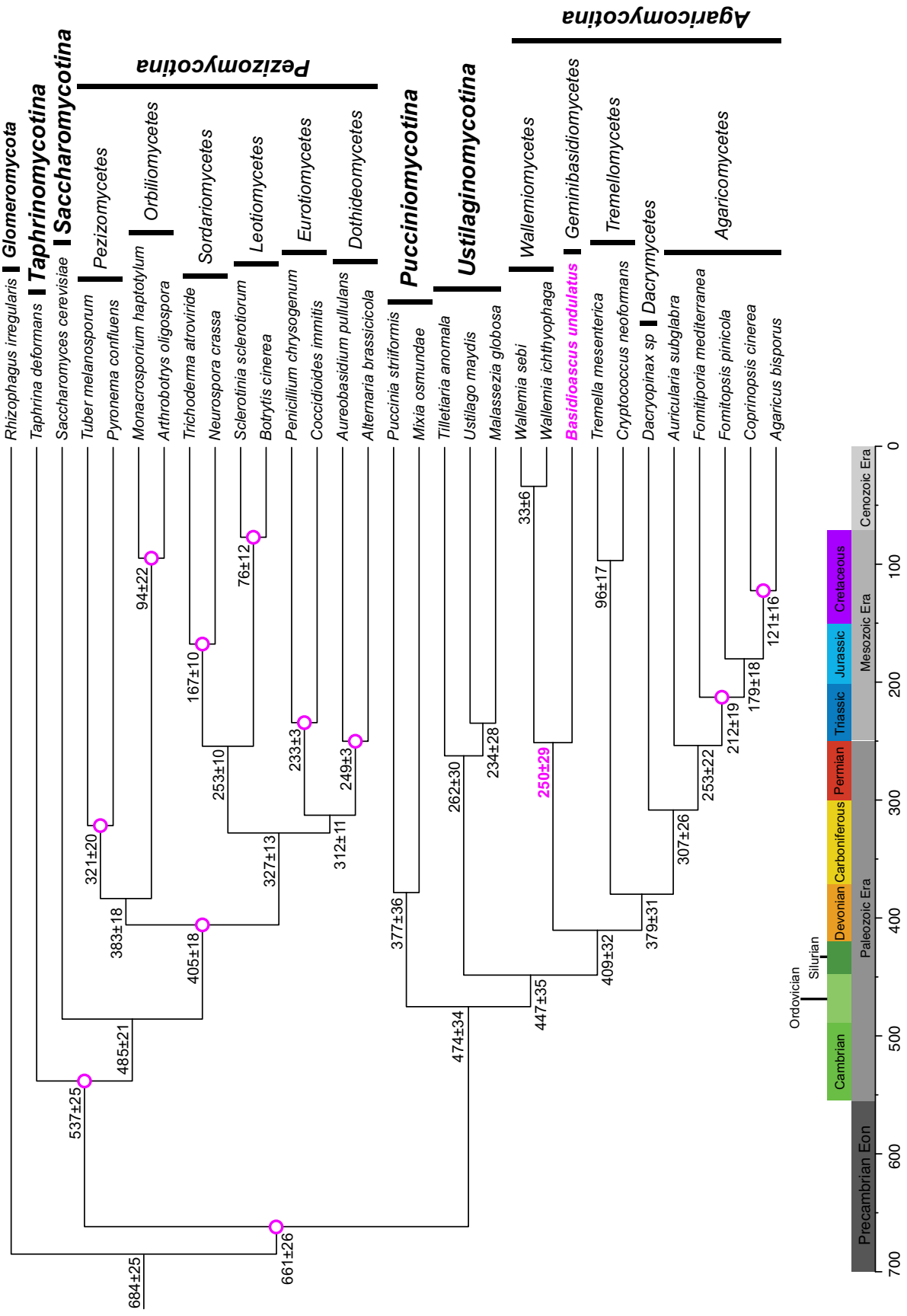


**Fig. 3.** Phylogenetic trees resulting from phylogenomic analysis and molecular dating. **A.** Consensus topology and branch lengths from analyses of concatenated amino acid sequences from 35 single copy genes with a total of 10129 data columns. Gapped and poorly aligned sites were removed. Analyses were performed with the CAT-GTR model. Posterior probabilities are shown at the nodes of the tree. Scale bar indicates expected changes per site. **B.** Chronogram resulting from a lognormal relaxed molecular clock analysis with the birth-death prior. The mean divergence time with standard error are shown at each node. Circled nodes were pre-calibrated before the analysis. The paleontological periods, in million years ago (Mya), are shown as a scale at the bottom. *Rhizophagus irregularis* (*Glomeromycota*) was used as the outgroup.

**Table 3.** Genome assembly and annotation statistics of *Basidioascus undulatus* compared to *Wallemia sebi* and *W. Ichthyophaga*.

| Descriptive statistic | *B. undulatus* | *W. sebi* | *W. icthyophaga* |
|---|---|---|---|
| **Genome assembly** | | | |
| Sequencing platform | Illumina Hi-Seq | Illumina Hi-Seq & 454 | Illumina Hi-Seq |
| Total number of reads | 12 Million[a] | — | — |
| Read length after trimming | 93 bp | — | — |
| Data size | 1.1 Gb | — | 3.7 Gb |
| Assembly size | 32 Mb[c] | 9.8 Mb | 9.6 Mb |
| Estimated Percent GC | 58%[c] | 40% | 45% |
| Nucleotide coverage | 24X[b] | 71X | >270X |
| Number of contigs | 3058 | 114 | 95 |
| Number of scaffolds | 2992 | 56 | 82 |
| Longest scaffold size | 97 Kb[c] | 900 Kb | 790 Kb |
| N50 | 15 Kb[c] | 340 Kb | 440 Kb |
| **Genome annotation** | | | |
| Percent core eukaryotic genes detected | 88%[d] | — | — |
| All predicted gene models | 13935[e] | 5284 | 4863 |
| Evidence supported gene models | 6123[e] | — | — |
| Evidence supported complete gene models | 3681 | — | — |

Statistics were found by the following programs: (a) FastQC,( b) qualimap, (c) QUAST, (d) CEGMA, and (e) MAKER.

protein sequences from completed fungal genome projects, was aligned to our *B. undulatus* genome using the program "exonerate". In the MAKER2 pipeline, aligning protein sequences to predicted genes on the genome generates 'evidence' expressed as the Annotation Evidence Distance (AED) score for exons (eAED) (Eilbeck *et al.* 2009). The eAED score is a metric that measures how a predicted gene determined from GeneMark-ES agrees with the protein alignment evidence from exonerate while accounting for protein reading frames shifts. This score is helpful for assessing annotation quality of a predicted gene (Eilbeck *et al.* 2009). Overall, 13 935 genes were predicted by GeneMark-ES but only 6123 of those genes were supported by protein alignment evidence. For each of the 6123 predicted genes, we made further functional annotation with a BLAST search against the UniProt/Swiss-Prot manually curated data set and an InterProScan analysis. Using this information, 452 genes were manually annotated with confidence. Future releases of the *B. undulatus* genome with RNA sequence data would increase the number of annotated genes and allow discovery and validation of completely novel genes or splice variants.

## Meiosis

We used genomic information in combination with confocal microscopy to gain further understanding of sexuality in *Basidioascus undulatus*. Fungal taxonomists infer function of meiosporangia in newly discovered fungi based on morphological similarities to proven meiosporangia in similar or related fungi. Proof of meiosis by nuclear staining is not usually required. In our case, *B. undulatus* is different morphologically, ontogenetically, and phylogenetically from known basidiomycetes and it was difficult to assess whether previous morphological interpretations by Nguyen *et al.* (2013) were correct without nuclear staining experiments. We suggested previously that the clavate structures found on somatic hyphae were basidia (Nguyen *et al.* 2013). These basidia were deciduous, forcibly discharged, and had a basal lateral projection that eventually collapsed. Sterigmata grew on the basidium, and a basidiospore developed at the tip of each sterigma. To verify these interpretations, we visualized these putative sexual structures with nuclear staining and confocal microscopy. Our observations suggested that meiosis occurred in the clavate structures (Fig. 1) providing the evidence for previous interpretation of them as basidia. Post-meiotic mitosis in the basidium was not seen but it was difficult to visualize nuclei in the mature basidiospores. Although we saw evidence of meiosis with microscopy, we also confirmed the presence of meiotic genes in the genome (Table 1). We did not detect *HOP*2 among the 10 meiosis specific genes. The *HOP*2 gene product is involved in preventing synapsis between non-homologous chromosomes during meiotic double-strand break repair (Malik *et al.* 2008). The function of *HOP*2 could be served by another unknown gene or gene product in *B. undulatus,* or perhaps our genome assembly was not complete enough to detect it. With 88 % of CEGs detected, about 1 out of every 10 genes would not be detected during the annotation procedure.

*Basidioascus undulatus* produces cells attached in chains, which are presumed to be arthroconidia (Nguyen *et al.* 2013). These arthroconidia were indeed single-nucleated (Fig. 1K–L) and therefore represent an asexual morph of *B. undulatus*. Given these results, *B. undulatus* indeed exhibits both sexual and asexual morphs in culture.

## Mating

The genes located at the MAT locus orchestrate the fungal mating process and determine the sex of individuals (Lee *et al.* 2010). In the fungal kingdom, mating is most comprehensively studied in *Saccharomyces cerevisiae*. Therefore, we used what is known about mating in *S. cerevisiae* as a model to

guide our interpretations of mating genes in the *B. undulatus* genome.

Homeodomain (HD) transcription factors control the expression of pheromone and pheromone receptor genes. Normally, dimerization occurs between two paralogous HD transcription factors, HD1 and HD2, to form HD1-HD2 complex. In *Ustilago maydis*, this is termed the bE/bW heterodimer, and in *S. cerevisiae* the a1/α2 complex (Lee *et al.* 2010). We identified the HD1 (8946F71C4C) and HD2 (AF24C22F02) proteins in *B. undulatus*.

Pheromone production and processing are also important in mating. All orthologs for pheromone processing (*KEX*1, *KEX*2, *STE*13, *RAM*1, *RAM*2, *STE*14, *AXL*11, *STE*6) were detected in *B. undulatus* except for the *RCE*1/*STE*24 genes responsible for cleavage of the pheromone peptide (Table 2).

Upon release into the environment, pheromones must bind to pheromone receptors to initiate a signaling cascade involving the mitogen-activated protein kinase (MAPK) pathway to turn on mating genes (Jones & Bennett 2011). MAPK pathways regulate the activity of high mobility group (HMG) DNA binding proteins, which are transcription factors regulating pheromone responsive genes in the MAT loci (Hartmann *et al.* 1996). Most of the mating response genes were detected (*STE*3, *KSS*1, *FUS*3, *STE*7, *STE*11, *GPA*1, *STE*4, *STE*20) (Table 2) except the G-protein γ subunit (*STE*18), the transcription factor *STE*12, the coordinator of MAPK pathway *STE*5, and the cell cycle control *FAR*1 protein. We identified four HMG DNA binding proteins (B013112742, C8B77D01D8, C1AD40EA22, and 9CC40B0A26).

We were unable to isolate single arthroconidia or successfully germinate basidiospores so mating tests were not possible. Thus, it is unknown whether *B. undulatus* is homothallic or heterothallic. *Wallemia sebi* apparently has a bipolar mating system (Padamsee *et al.* 2012) but no discernable mating type locus could be identified in the genome of *W. ichthyophaga* (Zajc *et al.* 2013). Our genome assembly was too fragmented to determine the structure of the mating type locus conclusively and therefore the mating system in *B. undulatus* remains uncharacterized until more sequencing is done. The detection of a near complete cellular machinery for the mating response, pheromone processing, and meiosis suggests that *B. undulatus* is capable of outcrossing. However, future experiments with gene knockout mutants will be needed to validate these identified genes.

## Higher classification and divergence of *Geminibasidiales*

*Basidioascus undulatus* and *Geminibasidium donsium* have been classified in *Geminibasidiales*, a sister order to *Wallemiales*. *Geminibasidiales* was placed tentatively in the class *Wallemiomycetes* (Nguyen *et al.* 2013). The main reason for this initial inconclusive placement was the absence of septal pore ultrastructure data and that only ribosomal genes could be used to make a phylogenetic analysis with enough taxon sampling to reach a conclusion. More genomes are available now and phylogenomic analysis with protein coding genes is more feasible and informative.

Our phylogenomic analysis shows the same relationships previously determined with rDNA, where *Wallemia* and *Basidioascus* are distantly related sister groups that occupy a basal phylogenetic position in *Agaricomycotina* (Fig. 3A). The distance of this relationship is also reflected in differences in GC content and genome size between *B. undulatus* and *Wallemia* discussed above. According to the sampling and assumptions made in our analyses, molecular dating suggests that the split between *B. undulatus* and *W. sebi* occurred 250 Mya (Fig. 3B), which is around the same time that *Sordariomycetes* split from *Leotiomycetes* (253 Mya) and *Exobasidiomycetes* from the *Ustilaginomycetes* and *Malasseziomycetes* (262 Mya), but we also note that not all nodes corresponding to class ranks in our analysis represent divergences at around 250 Mya. If our dates are accurate, it means *Wallemia* and *B. undulatus* shared a common ancestor until a divergence event occurred between the Permian and Triassic period. Interestingly, it was during this period that Earth experienced its most severe extinction event (Sahney & Benton 2008). The split between *W. sebi* and *W. ichthyophaga* was dated at 33±6 Mya, an estimate that differs from previous analyses; a 11.9 Mya split was proposed by Zajc *et al.* (2013), but with different methods, taxon sampling, and calibrations used for the molecular dating analysis. These estimates should all be considered approximate because the fungal fossil record is rather limited and many studies generate radically different age estimates for the same divergence events (Lücking *et al.* 2009).

Before sequence data began to dominate fungal systematics, morphological characters of the septa and septal pore caps were considered important for classifying fungi at the class or higher taxonomic levels (Khan & Kimbrough 1982, Oberwinkler & Bandoni 1982, Müller *et al.* 2000, van Driel *et al.* 2009) and septal pore morphology is still considered essential for delimiting classes in *Basidiomycota*. However, the overall septal pore morphologies of *B. undulatus* and *G. donsium* are similar and there are significant differences when compared to *W. sebi* (see p. 219 above; Fig. 2). The septal pore cap is probably not a reliable or practical feature for the classification of *Wallemia*, *Basidioascus* and *Geminibasidium* because it is sometimes present or absent in *Wallemia* (Padamsee *et al.* 2012, D.J. McLaughlin pers. comm.) and was not seen in *B. undulatus* or *G. donsium*.

Given the results obtained from phylogenomics analysis, molecular dating, and septal pore ultrastructure, we propose to classify *Geminibasidiales* in a new class *Geminibasidiomycetes*. Although *Geminibasidium* could not be included in the phylogenomic analysis and molecular dating because its genome is not yet sequenced, we are confident from previous rDNA phylogenetic analysis (Nguyen *et al.* 2013), morphological characters, and similarities in the septal pore morphology (Fig. 2) that *Geminibasidium* will remain a close sister group to *Basidioascus*. Previous phylogenies position *Wallemiomycetes* at the base of *Basidiomycota* (Matheny *et al.* 2006, Zalar *et al.* 2005), as a sister group to or as the earliest diverging lineage of *Agaricomycotina* (Padamsee *et al.* 2012, Nguyen *et al.* 2013, Zajc *et al.* 2013). The classification for the *Wallemiomycetes* is shown as *incertae sedis* in the *Basidiomycota* in the NCBI taxonomy (Federhen 2012), MycoBank (Robert

*et al.* 2013), and the Encyclopedia of Life (http://www.eol.org). In the taxonomic section below, we emend the description of the subphylum *Agaricomycotina* to include the classes *Geminibasidiomycetes* and *Wallemiomycetes* along with the *Agaricomycetes*, *Tremellomycetes* ,and *Dacrymycetes*, which are well delimited classes of *Agaricomycotina* (Hibbett 2007). By formally connecting the basal *Geminibasidiomycetes* and *Wallemiomycetes* to the *Agaricomycotina*, we eliminate the uncertain status of these taxa. The subphylum name *Wallemiomycotina* (MycoBank no. MB 550364) was published recently to accommodate *Wallemia* (Doweld 2014). There was no discussion of the rationale behind this proposal and we consider it unnecessary to include *Wallemiomycetes* (with or without the *Geminibasidiomycetes*) in its own subphylum.

## TAXONOMY

**Agaricomycotina** Doweld, *Prosyllabus*: lxxxvii (2001).
MycoBank MB560553
*Homonym*: *Agaricomycotina* R. Bauer *et al.*, *Mycol. Prog.* **5**: 45 (2006).

*Description*: Members of the *Basidiomycota* that have a cell wall carbohydrate composition with a dominance of glucose and presence of xylose and having a type B secondary structure of the 5S RNA (Bauer *et al.* 2006). Fungi that belong to this subphylum are classified in the classes *Agaricomycetes*, *Dacrymycetes*, *Tremellomycetes*, *Wallemiomycetes* or *Geminibasidiomycetes*.

*Notes*: Although *Agaricomycotina* Dowell (2001) is the oldest name, it is the concept of proposed by Bauer *et al.* (2006) (i.e. *Hymenomycetes sensu* Swann & Taylor 1995) that is widely used today. We modified it above only to explicitly state all of the accepted classes within *Agaricomycotina*. The cell wall of *B. persicus* was composed mostly of glucose and xylose (Nasr *et al.* 2014), and assuming that this is the same for other species of *Basidioascus* and *Geminibasidium*, this placement for the class *Geminibasidiomycetes* is appropriate. The cell wall carbohydrate composition of *Wallemia* species is unknown.

**Wallemiomycetes** Zalar *et al.*, *Antonie van Leeuwenhoek* **87**: 322 (2005).
MycoBank MB501496

*Description*: Class of xerophilic basidiomycetes belonging to the subphylum *Agaricomycotina*. These fungi produce basauxic anamorphs and do not produce basidiomata in culture. Species have dolipore septa with adseptal tubular extensions that arise from sheets of endoplasmic reticulum that form the septal pore cap. The septal pore cap is sometimes absent. The septal pore has an electron-dense non-membranous septal pore occlusion and striations that are oriented vertically.

*Type order*: *Wallemiales*.

*Notes*: This description is altered to exclude characters of *Geminibasidiales* previously added to the concept of *Wallemiomycetes* by Nguyen *et al.* (2013). Information about the septal pore morphology was added, as detailed in Padamsee *et al.* (2012).

**Geminibasidiomycetes** H.D.T. Nguyen & Seifert, **cl. nov.**
MycoBank MB811680

*Description*: Class of xerotolerant basidiomycetes belonging to the subphylum *Agaricomycotina*. *Basidiomata* not produced in culture. *Basidia* arising from somatic hyphae or from swollen basidium-bearing cells (primary cells) with a basal lateral projection occurring either on the basidium or the swollen primary cell. *Basidiospores* symmetrical on sterigma, not forcibly discharged, and brown at maturity. *Arthroconidial* and/or yeast-like asexual morphs sometimes produced. Species have a dolipore septum that is electron-dense at the pore swelling with an electron-dense membranous septal pore occlusion. Some species are heat resistant.

*Type order*: *Geminibasidiales*.

## ACKNOWLEDGEMENTS

We thank Adrian Pelin and Zaky Adam for discussions on genome assembly, Michael Li for advice on genome annotation with MAKER2, Christine Lowe for guidance on doing phylogenic analyses with PhyloBayes, Keith Bradnam for running CEGMA, Charlotte Grace and Karen Fisher for help with TEM, Jeff Cullis for reviewing an early draft of the manuscript, Robert Riley and Igor Grigoriev for processing and uploading genomic data to the JGI MycoCosm portal, and the staff at the DNA Technologies Laboratory at the National Research Council Canada (Saskatoon) for library construction and Illumina sequencing. The US National Science Foundation (NSF) provided support through a collaborative research grant to R.W.R. (DEB-0732503). The Ontario government provided funding support through the Ontario Graduate Scholarship (OGS) to H.D.T. Nguyen.

## REFERENCES

Amselem J, Cuomo CA, van Kan JA, Viaud M, Benito EP, *et al.* (2011) Genomic analysis of the necrotrophic fungal pathogens *Sclerotinia sclerotiorum* and *Botrytis cinerea*. *PLoS Genetics* **7** (8): e1002230.

Bankevich A, Nurk S, Antipov D, Gurevich AA, Dvorkin M, *et al.* (2012) SPAdes: a new genome assembly algorithm and its applications to single-cell sequencing. *Journal of Computational Biology* **19**: 455–477.

Bauer R, Begerow B, Sampaio JP, Weiss M, Oberwinkler F (2006) The simple-septate basidiomycetes: a synopsis. *Mycological Progress* **5**: 41–66.

Berbee ML, Taylor JW (2010) Dating the molecular clock in fungi – how close are we? *Fungal Biology Reviews* **24**: 1–16.

Boetzer M, Henkel CV, Jansen HJ, Butler D, Pirovano W (2011) Scaffolding pre-assembled contigs using SSPACE. *Bioinformatics* **27**: 578–579.

Borodovsky M, Lomsadze A (2011) Eukaryotic gene prediction using GeneMark.hmm-E and GeneMark-ES. *Current Protocols in Bioinformatics*: unit–4.610.

Camacho C, Coulouris G, Avagyan V, Ma N, Papadopoulos J, *et al.* (2009) BLAST+: architecture and applications. *BMC Bioinformatics* **10**: 421.

Cantu D, Govindarajulu M, Kozik A, Wang M, Chen X, *et al.* (2011) Next generation sequencing provides rapid access to the genome of *Puccinia striiformis* f. sp. *tritici*, the causal agent of wheat stripe rust. *PLoS ONE* **6** (8): e24230.

Celio GJ, Padamsee M, Dentinger BT, Bauer R, McLaughlin DJ (2007) ["2006"] Assembling the Fungal Tree of Life: constructing the structural and biochemical database. *Mycologia* **98**: 850–859.

Cisse OH, Almeida JM, Fonseca A, Kumar AA, Salojarvi J, *et al.* (2013) Genome sequencing of the plant pathogen *Taphrina deformans*, the causal agent of peach leaf curl. *mBio* **4** (3): e00055-00013.

Conesa A, Gotz S, Garcia-Gomez JM, Terol J, Talon M, *et al.* (2005) Blast2GO: a universal tool for annotation, visualization and analysis in functional genomics research. *Bioinformatics* **21**: 3674–3676.

Domsch KH, Gams W, Anderson TH (1980) *Compendium of Soil Fungi*. London: Academic Press.

Doweld AB (2014) *Wallemiomycotina*. *Index Fungorum* **73**: 1.

Duncan EG, Galbraith MH (1972) Post-meiotic events in the *Homobasidiomycetidae*. *Transactions of the British Mycological Society* **58**: 387–392.

Eilbeck K, Moore B, Holt C, Yandell M (2009) Quantitative measures for the management and comparison of annotated genomes. *BMC Bioinformatics* **10**: 67.

Federhen S (2012) The NCBI Taxonomy database. *Nucleic Acids Research* **40** (Database issue): D136–143.

Floudas D, Binder M, Riley R, Barry K, Blanchette RA, *et al.* (2012) The Paleozoic origin of enzymatic lignin decomposition reconstructed from 31 fungal genomes. *Science* **336**: 1715–1719.

Galagan JE, Calvo SE, Borkovich KA, Selker EU, Read ND, *et al.* (2003) The genome sequence of the filamentous fungus *Neurospora crassa*. *Nature* **422**: 859–868.

Garcia-Alcalde F, Okonechnikov K, Carbonell J, Cruz LM, Gotz S, *et al.* (2012) Qualimap: evaluating next-generation sequencing alignment data. *Bioinformatics* **28**: 2678–2679.

Goffeau A, Barrell BG, Bussey H, Davis RW, Dujon B, *et al.* (1996) Life with 6000 genes. *Science* **274**: 546, 563–567.

Gostincar C, Ohm RA, Kogej T, Sonjak S, Turk M, *et al.* (2014) Genome sequencing of four *Aureobasidium pullulans* varieties: biotechnological potential, stress tolerance, and description of new species. *BMC Genomics* **15**: 549.

Gouy M, Guindon S, Gascuel O (2010) SeaView version 4: A multiplatform graphical user interface for sequence alignment and phylogenetic tree building. *Molecular Biology and Evolution* **27**: 221–224.

Grigoriev IV, Nikitin R, Haridas S, Kuo A, Ohm R, *et al.* (2014) MycoCosm portal: gearing up for 1000 fungal genomes. *Nucleic Acids Research* **42** (Database issue):D699–704.

Gurevich A, Saveliev V, Vyahhi N, Tesler G (2013) QUAST: quality assessment tool for genome assemblies. *Bioinformatics* **29** (8): 1072–1075.

Haas BJ, Zeng Q, Pearson MD, Cuomo CA, Wortman JR (2011) Approaches to fungal genome annotation. *Mycology* **2**: 118-141.

Halary S, Malik SB, Lildhar L, Slamovits CH, Hijri M, *et al.* (2011) Conserved meiotic machinery in *Glomus* spp., a putatively ancient asexual fungal lineage. *Genome Biology and Evolution* **3**: 950–958.

Hanaichi T, Sato T, Iwamoto T, Malavasi-Yamashiro J, Hoshino M, *et al.* (1986) A stable lead by modification of Sato's method. *Journal of Electron Microscopy* **35**: 304–306.

Hartmann HA, Kahmann R, Bolker M (1996) The pheromone response factor coordinates filamentous growth and pathogenicity in *Ustilago maydis*. *EMBO Journal* **15**: 1632–1641.

Hibbett D, Grimaldi D, Donoghue M (1997) Fossil mushrooms from Miocene and Cretaceous ambers and the evolution of *Homobasidiomycetes*. *American Journal of Botany* **84**: 981–991.

Hibbett DS (2007) ["2006"] A phylogenetic overview of the *Agaricomycotina*. *Mycologia* **98**: 917–925.

Hoch HC (1986) Freeze-substitution of fungi. In: *Ultrastructure Techniques for Microorganisms* (Aldrich HC, Todd WJ, eds): 183–212. New York: Plenum Press.

Holt C, Yandell M (2011) MAKER2: an annotation pipeline and genome-database management tool for second-generation genome projects. *BMC Bioinformatics* **12**: 491.

Howard RJ, O'Donnell KL (1987) Freeze substitution of fungi for cytological analysis. *Experimental Mycology* **11**: 250–269.

James TY, Sun S, Li W, Heitman J, Kuo HC, *et al.* (2013) *Polyporales* genomes reveal the genetic architecture underlying tetrapolar and bipolar mating systems. *Mycologia* **105**: 1374–1390.

Jones P, Binns D, Chang HY, Fraser M, Li W, *et al.* (2014) InterProScan 5: genome-scale protein function classification. *Bioinformatics* **30**: 1236–1240.

Jones SK jr, Bennett RJ (2011) Fungal mating pheromones: choreographing the dating game. *Fungal Genetics and Biology* **48**: 668–676.

Kamper J, Kahmann R, Bolker M, Ma LJ, Brefort T, *et al.* (2006) Insights from the genome of the biotrophic fungal plant pathogen *Ustilago maydis*. *Nature* **444** : 97–101.

Khan SR, Kimbrough JW (1982) A reevaluation of the basidiomycetes based upon septal and basidial structures. *Mycotaxon* **15**: 103–120.

Kirk PM, Cannon PF, Minter DW, Stalpers JA (2008) *Ainsworth & Bisby's Dictionary of the Fungi.* 10th edn. Wallingford: CABI Publishing.

Kubicek CP, Herrera-Estrella A, Seidl-Seiboth V, Martinez DA, Druzhinina IS, *et al.* (2011) Comparative genome sequence analysis underscores mycoparasitism as the ancestral life style of *Trichoderma*. *Genome Biology* **12** (4):R40.

Lagesen K, Hallin P, Rodland EA, Staerfeldt HH, Rognes T, *et al.* (2007) RNAmmer: consistent and rapid annotation of ribosomal RNA genes. *Nucleic Acids Research* **35**: 3100–3108.

Langmead B, Salzberg SL (2012) Fast gapped-read alignment with Bowtie 2. *Nature Methods* **9**:357–359.

Lartillot N, Philippe H (2004) A Bayesian mixture model for across-site heterogeneities in the amino-acid replacement process. *Molecular Biology and Evolution* **21**: 1095–1109.

Lartillot N, Lepage T, Blanquart S (2009) PhyloBayes 3: a Bayesian software package for phylogenetic reconstruction and molecular dating. *Bioinformatics* **25**: 2286–2288.

Lartillot N, Rodrigue N, Stubbs D, Richer J (2013) PhyloBayes MPI: phylogenetic reconstruction with infinite mixtures of profiles in a parallel environment. Systematic *Biology* **62**: 611–615.

Lee SC, Ni M, Li W, Shertz C, Heitman J (2010) The evolution of sex: a perspective from the fungal kingdom. *Microbiology and Molecular Biology Reviews* **74**: 298–340.

Li H, Handsaker B, Wysoker A, Fennell T, Ruan J, *et al.* (2009) The Sequence Alignment/Map format and SAMtools. *Bioinformatics* **25**: 2078–2079.

Loftus BJ, Fung E, Roncaglia P, Rowley D, Amedeo P, *et al.* (2005) The genome of the basidiomycetous yeast and human pathogen *Cryptococcus neoformans*. *Science* **307**: 1321–1324.

Lücking R, Huhndorf S, Pfister DH, Plata ER, Lumbsch HT (2009) Fungi evolved right on track. *Mycologia* **101**: 810–822.

Malik SB, Pightling AW, Stefaniak LM, Schurko AM, Logsdon JM jr. (2008) An expanded inventory of conserved meiotic genes provides evidence for sex in *Trichomonas vaginalis*. *PLoS ONE* **3** (8): e2879.

Marthey S, Aguileta G, Rodolphe F, Gendrault A, Giraud T, *et al.* (2008) FUNYBASE: a FUNgal phYlogenomic dataBASE. *BMC Bioinformatics* **9**: 456.

Martin F, Kohler A, Murat C, Balestrini R, Coutinho PM, *et al.* (2010) Perigord black truffle genome uncovers evolutionary origins and mechanisms of symbiosis. *Nature* **464**: 1033–1038.

Matheny PB, Gossmann JA, Zalar P, Kumar TK, Hibbett DS (2006) Resolving the phylogenetic position of the *Wallemiomycetes*: an enigmatic major lineage of *Basidiomycota*. *Canadian Journal of Botany* **84**: 1794–1805.

Matsushima T (2003) *Basidioascus* gen. nov. *Matsushima Mycological Memoirs* **10**: 98–104.

McDaniel DP, Roberson RW (2000) Intracellular motility and mechanisms of control during hyphal tip growth in *Allomyces*. *Fungal Genetics and Biology* **31**: 223–234.

Meerupati T, Andersson KM, Friman E, Kumar D, Tunlid A, *et al.* (2013) Genomic mechanisms accounting for the adaptation to parasitism in nematode-trapping fungi. *PLoS Genetics* **9** (11): e1003909.

Misiek M, Hoffmeister D (2008) Processing sites involved in intron splicing of *Armillaria* natural product genes. *Mycological Research* **112**: 216–224.

Morin E, Kohler A, Baker AR, Foulongne-Oriol M, Lombard V, *et al.* (2012) Genome sequence of the button mushroom *Agaricus bisporus* reveals mechanisms governing adaptation to a humic-rich ecological niche. *Proceedings of the National Academy of Sciences, USA* **109**: 17501–17506.

Müller WH, Stalpers JA, van Aelst AC, de Jong MDM, van der Krift TP, *et al.* (2000) The taxonomic position of *Asterodon*, *Asterostroma* and *Coltricia* inferred from the septal pore cap ultrastructure. *Mycological Research* **104**:1485–1492.

Nasr S, Soudi MR, Nasrabadi SM, Nikou MM, Salmanian AH, *et al.* (2014) *Basidioascus persicus* sp. nov., a yeast-like species of the order *Geminibasidiales* isolated from soil. *International Journal of Systematic and Evolutionary Microbiology* **64**: 3046–3052.

Nguyen HDT, Nickerson NL, Seifert KA (2013) *Basidioascus* and *Geminibasidium*: a new lineage of heat-resistant and xerotolerant basidiomycetes. *Mycologia* **105**: 1231–1250.

Nikolenko SI, Korobeynikov AI, Alekseyev MA (2013) BayesHammer: Bayesian clustering for error correction in single-cell sequencing. *BMC Genomics* **14** (Suppl 1): S7.

Notredame C, Higgins DG, Heringa J (2000) T-Coffee: A novel method for fast and accurate multiple sequence alignment. *Journal of Molecular Biology* **302**: 205–217.

Oberwinkler F, Bandoni RJ (1982) A taxonomic survey of the gasteroid, auricularioid Heterobasidiomycetes. *Canadian Journal of Botany* **60**: 1726–1750.

Ohm RA, Feau N, Henrissat B, Schoch CL, Horwitz BA, *et al.* (2012) Diverse lifestyles and strategies of plant pathogenesis encoded in the genomes of eighteen *Dothideomycetes* fungi. *PLoS Pathogens* **8** (12): e1003037.

Padamsee M, Kumar TK, Riley R, Binder M, Boyd A, *et al.* (2012) The genome of the xerotolerant mold *Wallemia sebi* reveals adaptations to osmotic stress and suggests cryptic sexual reproduction. *Fungal Genetics and Biology* **49**: 217–226.

Parra G, Bradnam K, Korf I (2007) CEGMA: a pipeline to accurately annotate core genes in eukaryotic genomes. *Bioinformatics* **23**: 1061–1067.

Prieto M, Wedin M (2013) Dating the diversification of the major lineages of *Ascomycota* (*Fungi*). *PLoS ONE* **8** (6): e65576.

Rep M, Duyvesteijn RG, Gale L, Usgaard T, Cornelissen BJ, *et al.* (2006) The presence of GC-AG introns in *Neurospora crassa* and other euascomycetes determined from analyses of complete genomes: implications for automated gene prediction. *Genomics* **87**: 338–347.

Roberson RW, Fuller MS (1988) Ultrastructural aspects of the hyphal tip of *Sclerotium rolfsii* preserved by freeze substitution. *Protoplasma* **146**: 143–149.

Robert V, Vu D, Amor AB, van de Wiele N, Brouwer C, *et al.* (2013) MycoBank gearing up for new horizons. *IMA Fungus* **4**: 371–379.

Sahney S, Benton MJ (2008) Recovery from the most profound mass extinction of all time. *Proceedings of the Royal Society of London, Biological Sciences* **275** : 759–765.

Schneider CA, Rasband WS, Eliceiri KW (2012) NIH Image to ImageJ: 25 years of image analysis. *Nature Methods* **9**: 671–675.

Sharpton TJ, Stajich JE, Rounsley SD, Gardner MJ, Wortman JR, *et al.* (2009) Comparative genomic analyses of the human fungal pathogens *Coccidioides* and their relatives. *Genome Research* **19**: 1722–1731.

Sims D, Sudbery I, Ilott NE, Heger A, Ponting CP (2014) Sequencing depth and coverage: key considerations in genomic analyses. *Nature Reviews Genetics* **15**: 121–132.

Slater GS, Birney E (2005) Automated generation of heuristics for biological sequence comparison. *BMC Bioinformatics* **6**: 31.

Smith SY, Currah RS, Stockey RA (2004) Cretaceous and Eocene poroid hymenophores from Vancouver Island, British Columbia. *Mycologia* **96**:180–186.

Spurr AR (1969) A low-viscosity epoxy resin embedding medium for electron microscopy. *Journal of Ultrastructure Research* **26** (1):31–43.

Staats M, van Kan JA (2012) Genome update of *Botrytis cinerea* strains B05.10 and T4. *Eukaryotic Cell* **11**: 1413–1414.

Stajich JE, Wilke SK, Ahren D, Au CH, Birren BW, *et al.* (2010) Insights into evolution of multicellular fungi from the assembled chromosomes of the mushroom *Coprinopsis cinerea* (*Coprinus cinereus*). *Proceedings of the National Academy of Sciences, USA* **107**: 11889–11894.

Swann EC, Taylor JW (1995) Phylogenetic perspectives on basidiomycete systematics: evidence from the 18s rRNA gene. *Canadian Journal of Botany* **73** (S1): 862–868.

Taylor JW, Berbee ML (2007) ["2006"] Dating divergences in the Fungal Tree of Life: review and new analyses. *Mycologia* **98**: 838–849.

Ter-Hovhannisyan V, Lomsadze A, Chernoff YO, Borodovsky M (2008) Gene prediction in novel fungal genomes using an *ab*

*initio* algorithm with unsupervised training. *Genome Research* **18**: 1979–1990.

Terracina FC (1974) Fine structure of the septum in *Wallemia sebi*. *Canadian Journal of Botany* **52**: 2587–2590.

Tisserant E, Malbreil M, Kuo A, Kohler A, Symeonidi A, *et al.* (2013) Genome of an arbuscular mycorrhizal fungus provides insight into the oldest plant symbiosis. *Proceedings of the National Academy of Sciences, USA* **110**: 20117–20122.

Toome M, Kuo A, Henrissat B, Lipzen A, Tritt A, *et al.* (2014a) Draft genome sequence of a rare smut relative, *Tilletiaria anomala* UBC 951. *Genome Announcements* **2** (3): e00539-14.

Toome M, Ohm RA, Riley RW, James TY, Lazarus KL, *et al.* (2014b) Genome sequencing provides insight into the reproductive biology, nutritional mode and ploidy of the fern pathogen *Mixia osmundae*. *New Phytologist* **202**: 554–564.

Traeger S, Altegoer F, Freitag M, Gabaldon T, Kempken F, *et al.* (2013) The genome and development-dependent transcriptomes of *Pyronema confluens*: a window into fungal evolution. *PLoS Genetics* **9** (9): e1003820.

van den Berg MA, Albang R, Albermann K, Badger JH, Daran JM, *et al.* (2008) Genome sequencing and analysis of the filamentous fungus *Penicillium chrysogenum*. *Nature Biotechnology* **26**: 1161–1168.

van Driel KG, Humbel BM, Verkleij AJ, Stalpers J, Muller WH, *et al.* (2009) Septal pore complex morphology in the *Agaricomycotina* (*Basidiomycota*) with emphasis on the *Cantharellales* and *Hymenochaetales*. *Mycological Research* **113**: 559–576.

Xu J, Saunders CW, Hu P, Grant RA, Boekhout T, *et al.* (2007) Dandruff-associated *Malassezia* genomes reveal convergent and divergent virulence traits shared with plant and human fungal pathogens. *Proceedings of the National Academy of Sciences, USA* **104**: 18730–18735.

Yang J, Wang L, Ji X, Feng Y, Li X, *et al.* (2011) Genomic and proteomic analyses of the fungus *Arthrobotrys oligospora* provide insights into nematode-trap formation. *PLoS Pathogens* **7** (9): e1002179.

Zajc J, Liu Y, Dai W, Yang Z, Hu J, *et al.* (2013) Genome and transcriptome sequencing of the halophilic fungus *Wallemia ichthyophaga*: haloadaptations present and absent. *BMC Genomics* **14**: 617.

Zalar P, de Hoog GS, Schroers HJ, Frank JM, Gunde-Cimerman N (2005) Taxonomy and phylogeny of the xerophilic genus *Wallemia* (*Wallemiomycetes* and *Wallemiales*, cl. et ord. nov.). *Antonie van Leeuwenhoek* **87**: 311–328.